High Ion Temperature Plasmas using an ICRF Wall-Conditioning Technique in the Large Helical Device

Hiromi TAKAHASHI, Masaki OSAKABE, Sadayoshi MURAKAMI[1], Kenichi NAGAOKA,
Haruhisa NAKANO, Yasuhiko TAKEIRI, Tetsuo SEKI, Kenji SAITO, Hiroshi KASAHARA,
Shuji KAMIO, Takashi MUTOH and the LHD Experiment Group

National Institute for Fusion Science, 322-6 Oroshi-cho, Toki 509-5292, Japan
[1]*Department of Nuclear Engineering, Kyoto University, Kyoto 606-8501, Japan*

A new effective wall-conditioning technique was proposed for realizing high ion temperature (T_i) plasmas in the Large Helical Device using the ion cyclotron range of frequency (ICRF) wave under the established magnetic confinement field. A series of ICRF heating discharges using He as the working gas was conducted ahead of the high-T_i plasma discharges. After sufficient repetitive wall-conditioning discharges, we observed a decrease in the line-averaged electron density, the formation of a peaked electron density profile, a reduction in the Hα emission, and an increase in the central T_i. The results suggest that the stored hydrogen inside the vacuum vessel structures, such as the first wall, the diverter, and other components, sputtered out owing to the He plasmas of the ICRF wall-conditioning discharges and the hydrogen recycling was decreased. Consequently, the ion heating power of NBI increased in the plasma core region, leading to higher central T_i.

1. Introduction

The wall conditions substantially affect the plasma performance in the toroidal system [1–7]. In the Large Helical Device (LHD), high-performance plasmas such as super-dense core plasmas and high ion temperature (T_i) plasmas have been realized owing to peripheral particle control techniques such as the local island diverter, glow discharges, and titanium gettering [8–10]. Recently, high-T_i plasmas, which were produced using high-power NBIs, were obtained using a series of wall-conditioning discharges of the 38-MHz ion cyclotron range of frequency (ICRF) wave ahead the high-T_i plasma discharges [11]. In typical high-T_i plasmas in the LHD, hollow electron density (n_e) profiles have been observed. In contrast, a peaked n_e profile and higher T_i were obtained after the ICRF wall-conditioning discharges.

In this study, we discuss the effect of the ICRF wall-conditioning on the production of high-T_i plasmas in the LHD. First, the new wall-conditioning technique using the ICRF wave is introduced. Next, the production of the high-T_i plasmas using the ICRF wall-conditioning technique is presented. The effect of the ICRF discharges on the reduction of hydrogen recycling from the vacuum vessel components is discussed. Finally, the results are summarized.

2. ICRF Wall-Conditioning under the Established Confinement Magnetic Field

The LHD is the largest heliotron device in the world with a major radius of 3.9 m, a minor radius of 0.6 m, a pole number of 2, and a toroidal period of 10 [12–14]. The heliotron configurations are produced by a set of helical
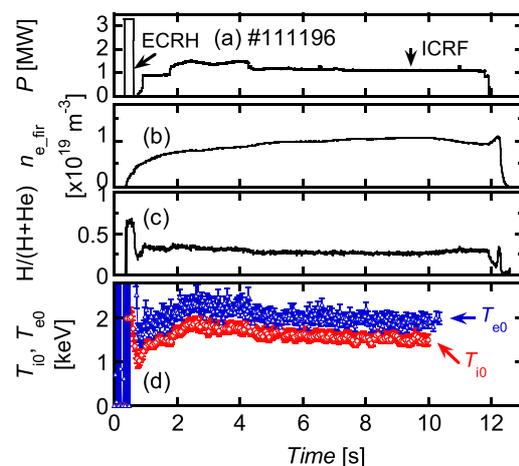

Fig. 1 Typical time evolution of (a) the heating power of the ICRF wave and ECRH, (b) the line-averaged electron density n_{e_fir}, (c) the H/(H + He) value, and (d) the central temperature of ion T_{i0} and electron T_{e0}.
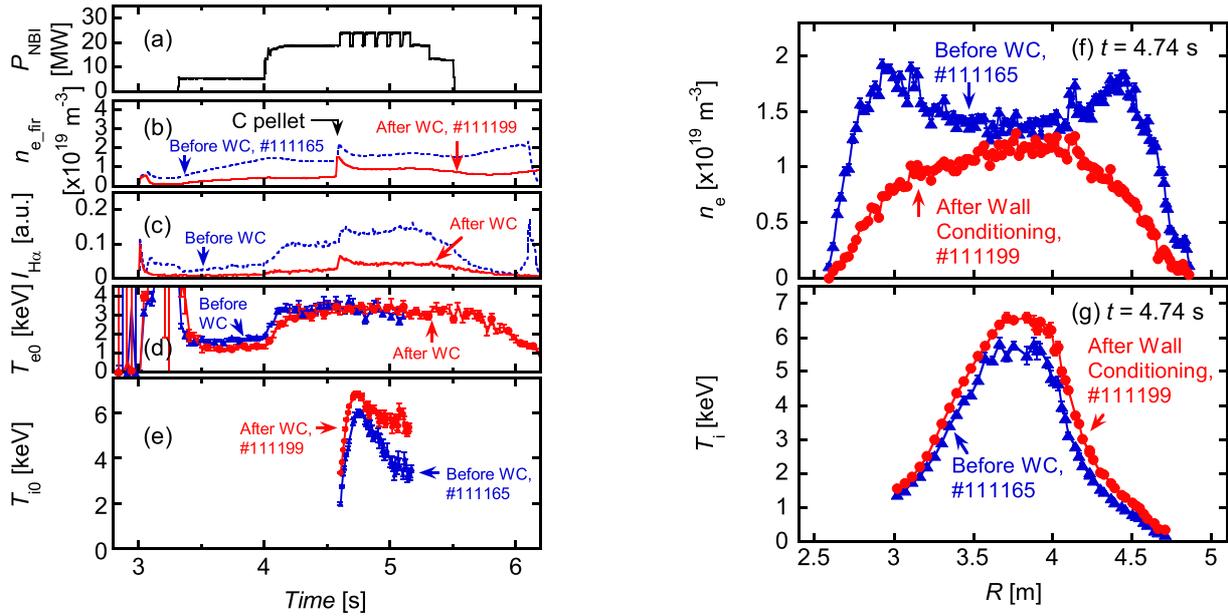
Fig. 2   Time evolution of (a) the NBI port through power P_{NBI}, (b) n_{e_fir}, (c) Hα emission intensity $I_{H\alpha}$, (d) T_{e0}, (e) T_{i0}, the radial profiles of (f) n_e, and (g) T_i at $t = 4.74$ s for the high-T_i discharges just before (#111165) and after (#111199) the ICRF wall-conditioning.

coils and three sets of poloidal field coils, which are all superconducting magnets. Therefore, the steady-state formation of magnetic configuration and plasma sustainment are realized. The magnetic field on the axis is ~2.9 T.

The new wall-conditioning discharges using the ICRF wave were conducted ahead of the high-T_i discharges. Figure 1 shows the typical time evolution of (a) the heating power of the ICRF wave and electron-cyclotron resonance heating (ECRH), (b) the line-averaged electron density n_{e_fir}, (c) the H/(H + He) value [15], and (d) the central temperature of ion T_{i0} and electron T_{e0}. The discharge was conducted using He as the working gas for the ICRF heating under the established confinement magnetic field of $R_{ax} = 3.6$ m, $|B_t| = 2.75$ T. The plasma was ignited using 3 MW ECRH and was steadily sustained with n_e of $0.7 - 1 \times 10^{19}$ m^{-3} using 38-MHz ICRF heating only for 12 s. Low value of an H/(H + He) is suitable for the effective hydrogen minority heating of the ICRF wave. Although the plasma was maintained during the ICRF wave injection, T_{i0} and T_{e0} are shown up to 10 s owing to data acquisition limitations. The preferred conditions for high-T_i plasmas are realized after several tens ICRF wall-conditioning discharges.

3. Effect of the ICRF Wall Conditioning on the High-T_i plasma Performance

Figure 2 shows the time evolution of (a) the NBI port through power P_{NBI}, (b) n_{e_fir}, (c) Hα emission intensity $I_{H\alpha}$, (d) T_{e0}, (e) T_{i0}, (f) radial profiles of n_e, and (g) T_i at $t = 4.74$ s for the high-T_i discharges just before (#111165)

and after (#111199) the ICRF wall conditioning. Between the two discharges, 30 ICRF conditioning discharges were conducted. In the LHD, high-T_i plasmas are typically produced using high-power NBI and carbon pellets [10, 11]. A column-shaped carbon pellet ($\phi 1.0$ mm $\times$ $l 1.0$ mm) was injected at $t = 4.52$ s and n_{e_fir} increased sharply. In the density decay phase, T_{i0} increased until ~4.75 s and then gradually decreased. In the plasma, just after the ICRF conditioning discharges, we observed a decrease in the averaged density, high T_i, a clear reduction in the Hα signal, and a change in the n_e profile from hollow to peaked. The reduction in Hα represents a decrease in hydrogen recycling from in-vessel components. The change in the n_e profile is due to the decrease in hydrogen recycling. Consequently, the NBI absorption power per ion increased in the plasma core region leading to the high-T_i plasma [11].

Figure 2 also shows the wall-conditioning effect for the different methods. Before starting the experiment, two-hour He glow discharge and 4-hour titanium gettering were performed. Discharge #111165 was obtained early in the day (fifth shot), and thus was considered to have substantially benefited from the wall conditionings. Comparing the attained T_{i0} in the discharges, just after the different wall-conditioning methods, the ICRF wall conditioning in the established magnetic field was found more effective than the conventional wall-conditioning technique for realizing high-T_i plasmas.

4. Discussion

Figure 3 shows the time trend of (a) the hydrogen pressure P_{H2} inside the LHD, (b) T_{i0} at $t = 4.74$ s and the integration of the input ICRF energy W_{ICRF} during a typical
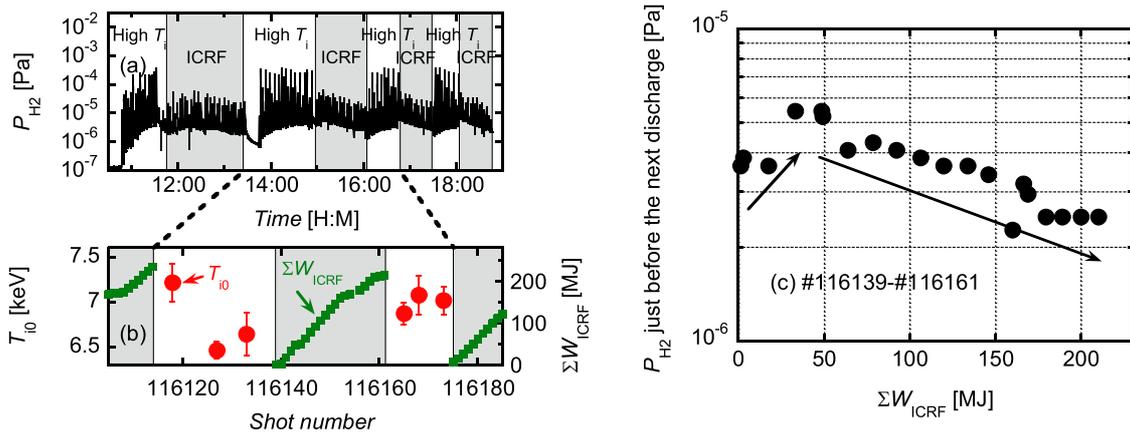
Fig. 3 Time trend of (a) the hydrogen pressure P_{H2} inside the LHD, (b) T_{i0} at $t = 4.74$ s and the integration of the input ICRF energy W_{ICRF} in an LHD experiment day and (c) the relation between ΣW_{ICRF} and P_{H2} just before the next ICRF discharge.
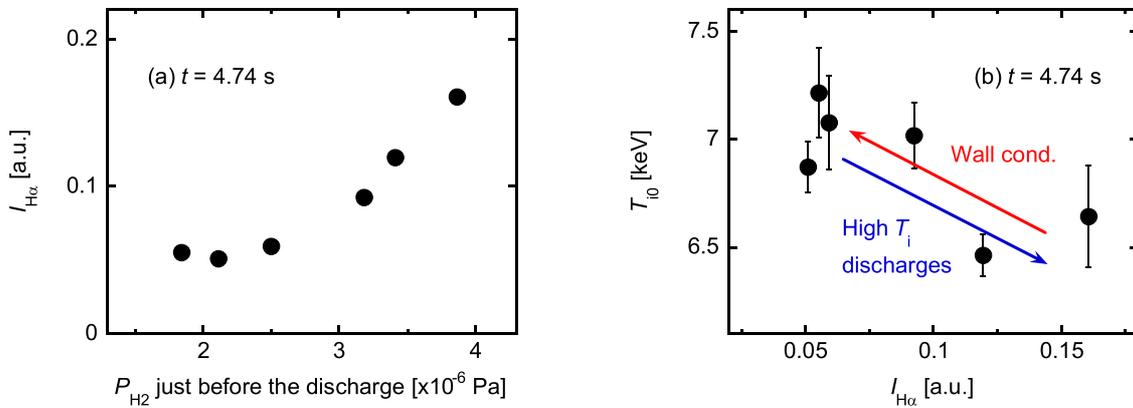

Fig. 4 Dependence of (a) $I_{H\alpha}$ on P_{H2} just before the discharge and (b) T_{i0} on $I_{H\alpha}$ for the six high-T_i discharges in Fig. 3 (b).

LHD experiment day, and (c) the relation between ΣW_{ICRF} and P_{H2} just before the next ICRF discharge. The horizontal axis in Fig. 3 (b) is an expansion of that in Fig. 3 (a) and represents the corresponding shot number. The W_{ICRF} value is the product of the ICRF heating power and the pulse length. The ICRF wall-conditioning discharges were conducted in the hatched period. As seen in Figs. 3 (a) and 3 (b), although plasma with $T_{i0} > 7$ keV could be produced just after the ICRF wall conditioning, the residual hydrogen pressure inside the LHD vacuum vessel gradually increased (please see the bottom envelope of Fig. 3 (a)) as the high-T_i discharges continued and the attained T_{i0} decreased. Then, several tens of ICRF wall-conditioning discharges were conducted and T_{i0} exceeding 7 keV was obtained again. During the ICRF wall conditioning, the residual hydrogen pressure increased in the initial discharges up to a ΣW_{ICRF} of 50 MJ and then decreased with increasing ΣW_{ICRF} (Fig. 3 (c)). This is evidence that the hydrogen gas stored inside the vacuum vessel components sputtered out because of the ICRF-He plasma.

Figure 4 shows the dependence of (a) $I_{H\alpha}$ on P_{H2} just before the discharge and (b) T_{i0} on $I_{H\alpha}$ for the six high-T_i

discharges shown in Fig. 3 (b). The $H\alpha$ emission decreased with decreasing residual hydrogen pressure before the discharge and the attained T_{i0} increased with decreasing $H\alpha$ emission.

The above results suggest that (1) wall recycling clearly decreased owing to the hydrogen sputtered from the wall because of the ICRF-He discharges, and (2) low-recycling conditions are critical for realizing high-T_i plasmas.

Similar favorable effects of ECRH instead of ICRF wall-conditioning for realizing high-T_i plasma were observed in the last LHD experimental campaign. In the experiments, several tens of ECRH discharges using He gas were conducted ($\Sigma W_{ECRH} \sim 300$ MJ) before the high-T_i discharges, reduction in the $H\alpha$ emission, and high T_i were observed. These results imply that not only the high-energy particle flux produced by ICRF but also the total input energy of the RF wave is important for low wall-recycling conditions.

Recently, an experiment to investigate the ICRF-He plasma effect on the microscopic characteristics of the vacuum vessel component was conducted. In this experiment,

small specimens composed of graphite and stainless steel (SUS316), which are the materials of the diverter and the first wall of the LHD, respectively, were set at the first wall position using a material probe system [16] and were irradiated with a series of ICRF-He plasmas. The experiment will help clarify how the ICRF wall conditioning and the produced high-energy particles affect the hydrogen sputtering characteristics, microscopic modification of the surface, and interior atomic structure of the vacuum vessel components.

5. Summary

A new effective wall-conditioning technique was established in the LHD for high-T_i plasmas using the ICRF wave under the established magnetic confinement field. After several repetitive wall-conditioning discharges, we observed a decrease in the line-averaged n_e, the formation of a peaked n_e profile, a reduction in the Hα emission, and an increase in the central T_i. The results suggest that the stored hydrogen inside the vacuum vessel structures sputtered out because of the He plasmas of the ICRF wall-conditioning discharges and hydrogen recycling decreased. Consequently, the ion heating power of the NBI increased in the plasma core region, leading to high central T_i [11]. By comparing the attained T_{i0} in the discharges, just after the different wall-conditioning methods, we find that the ICRF wall conditioning in the established magnetic field is more effective for realizing high-T_i plasmas than the conventional wall-conditioning technique in the LHD, i.e., He glow discharge and titanium gettering. The effect of the ICRF wall-conditioning discharges on the microscopic modification of the vacuum vessel components will be presented in the near future.

[1] A. Sagara *et al.*, J. Plasma Fusion Res. **39**, 1245 (1999).
[2] D. Tafalla and F.L. Tabares, J. Nucl. Mater. **290-293**, 1195 (2001).
[3] K. Nishimura *et al.*, J. Plasma Fusion Res. **79**, 1216 (2003).
[4] K. Nishimura *et al.*, J. Nucl. Mater. **337-339**, 431 (2005).
[5] E. De Lacal and E. Gauthier, Plasma Phys. Control. Fusion **47**, 197 (2005).
[6] V. Rohde *et al.*, J. Nucl. Mater. **363-365**, 1369 (2007).
[7] S. Masuzaki *et al.*, Fusion Sci. Technol. **58**, 297 (2010).
[8] N. Ohyabu *et al.*, Phys. Rev. Lett. **97**, 055002 (2006).
[9] A. Komori *et al.*, J. Nucl. Mater. **390-391**, 232 (2009).
[10] K. Nagaoka *et al.*, Nucl. Fusion **51**, 083022 (2011).
[11] H. Takahashi *et al.*, Nucl. Fusion **53**, 073034 (2013).
[12] H. Yamada *et al*., Fusion Sci. Technol. **58**, 12 (2010).
[13] H. Yamada for the LHD Experiment Group, Nucl. Fusion **51**, 094021 (2011).
[14] O. Kaneko *et al*., Nucl. Fusion **53**, 104015 (2013).
[15] S. Morita *et al.*, J. Plasma Fusion Res. **3**, S1037 (2008).
[16] M. Tokitani *et al.*, Nucl. Fusion **45**, 1544 (2005).